

# Effects of nuclear cross sections on $^{19}\text{F}$ nucleosynthesis at low metallicities (Research Note)

S. Cristallo<sup>1,2</sup>, A. Di Leva<sup>3,2</sup>, G. Imbriani<sup>3,2</sup>, L. Piersanti<sup>1,2</sup>, C. Abia<sup>4</sup>, L. Gialanella<sup>5,2</sup>, and O. Straniero<sup>1,2</sup>

<sup>1</sup> INAF, Osservatorio Astronomico di Collurania, 64100 Teramo, Italy  
e-mail: sergio.cristallo@inaf.it

<sup>2</sup> INFN Sezione Napoli, Napoli (Italy)

<sup>3</sup> Dipartimento di Fisica, Università di Napoli “Federico II”, Napoli, Italy

<sup>4</sup> Departamento de Física Teórica y del Cosmos, Universidad de Granada, 18071 Granada, Spain

<sup>5</sup> Dipartimento di Matematica e Fisica, Seconda Università di Napoli, Caserta, Italy

Received ; accepted

## ABSTRACT

**Context.** The origin of fluorine is a longstanding problem in nuclear astrophysics. It is widely recognized that Asymptotic Giant Branch (AGB) stars are among the most important contributors to the Galactic fluorine production.

**Aims.** In general, extant nucleosynthesis models overestimate the fluorine production by AGB stars with respect to observations. Although at solar metallicity those differences are rather small, low metallicity AGB stellar models predict fluorine surface abundances up to one order of magnitude larger than the observed ones.

**Methods.** As part of a project devoted to the reduction of the nuclear physics uncertainties affecting the nucleosynthesis in AGB stellar models, in this paper we review the relevant nuclear reaction rates involved in the fluorine production/destruction. We perform this analysis on a model with initial mass  $M=2 M_{\odot}$  and  $Z=0.001$ .

**Results.** We found that the major uncertainties are due to the  $^{13}\text{C}(\alpha,n)^{16}\text{O}$ , the  $^{19}\text{F}(\alpha,p)^{22}\text{Ne}$  and the  $^{14}\text{N}(p,\gamma)^{15}\text{O}$  reactions. A change of the corresponding reaction rates within the present experimental uncertainties implies surface  $^{19}\text{F}$  variations at the AGB tip lower than 10%, thus much smaller than observational uncertainties. For some  $\alpha$  capture reactions, however, cross sections at astrophysically relevant energies are determined on the basis of nuclear models, in which some low energy resonance parameters are very poorly known. Thus, larger variations in the rates of those processes cannot be excluded. That being so, we explore the effects of the variation of some  $\alpha$  capture rates well beyond the current published uncertainties. The largest  $^{19}\text{F}$  variations are obtained by varying the  $^{15}\text{N}(\alpha,\gamma)^{19}\text{F}$  and the  $^{19}\text{F}(\alpha,p)^{22}\text{Ne}$  reactions.

**Conclusions.** The currently estimated uncertainties of the nuclear reaction rates involved in the production and destruction of fluorine produce minor  $^{19}\text{F}$  variations in the ejecta of AGB stars. The analysis of some  $\alpha$  capture processes assuming a wider uncertainty range determines  $^{19}\text{F}$  abundances in better agreement with recent spectroscopic fluorine measurements at low metallicity. In the framework of the latter scenario the  $^{15}\text{N}(\alpha,\gamma)^{19}\text{F}$  and the  $^{19}\text{F}(\alpha,p)^{22}\text{Ne}$  reactions show the largest effects on fluorine nucleosynthesis. The presence of poorly known low energy resonances make such a scenario, even if unlikely, possible. We plan to directly measure these resonances.

**Key words.** Physical data and processes: nuclear reaction, nucleosynthesis, abundances; stars: AGB and post-AGB

## 1. Introduction

The production of fluorine ( $^{19}\text{F}$ ) is an intriguing and largely debated problems in stellar nucleosynthesis. Several stellar sites have been proposed as  $^{19}\text{F}$  factories: core-collapse Supernovae (Woosley & Haxton 1988), Wolf-Rayet stars (Meynet & Arnould 2000) and Asymptotic Giant Branch (AGB) stars (Forestini et al. 1992). While some papers excluded the first two scenarios (Federman et al. 2005; Palacios et al. 2005), more recent studies stressed the importance of both SuperNovae (Kobayashi et al. 2011) and Wolf-Rayet stars (Jönsson et al. 2014). Among all the proposed scenarios, however, a direct proof of fluorine production has been proved only

in AGB stars, via spectroscopic detections of  $[\text{F}/\text{Fe}]$  enhancements (see Abia et al. 2009 and references therein).

The first systematic search of fluorine enhancements in AGB stars was done by Jorissen et al. (1992), who measured abundances for red giants of type K, Ba, M, MS, S, SC, N and J of near solar metallicity. The result of this study was very high  $^{19}\text{F}$  surface enrichments (up to 30 times solar) in N type C-stars and a clear correlation between the fluorine enhancement and the C/O ratio. N-type C stars are low-mass stars close to the AGB tip. Although this occurrence was immediately interpreted as clear evidence of the fluorine synthesis by AGB stars, theoretical models failed in reproducing such a large surface fluorine enrichment (Forestini et al. 1992; Lugaro et al. 2004; Cristallo et al. 2009). However, a re-analysis

Send offprint requests to: S. Cristallo

made by Abia et al. (2009, 2010) of the same sample reconciled theoretical models with observations. A systematic reduction of fluorine abundances, by 0.7 dex on average, was found, relating this discrepancy to blends with C-bearing molecular lines not properly taken into account in Jorissen et al. (1992). As a matter of fact, at solar-like metallicities, the agreement between theory and observations is rather good. However, extant fluorine observational data may suffer a non negligible reduction due to an error in the adopted HF excitation energies of infrared lines (see Jönsson et al. 2014). This might systematically diminish the spectroscopic  $^{19}\text{F}$  estimates by 0.1 dex up to 0.5 dex in the cooler AGB stars.

At low metallicities, the situation is even more complex. Fluorine measurements in three extragalactic low metallicity ( $-2 < [\text{Fe}/\text{H}] < -1$ ) AGB stars (Abia et al. 2011) disagree with theoretical models, which predict fluorine surface abundances about an order of magnitude larger (see Cristallo et al. 2009, 2011, and also Figures 3 and 4 in Abia et al. 2011). On the other hand, these objects are largely enriched in s-process elements, with  $0.9 < \langle [s]/\text{Fe} \rangle^1 < 1.6$  (de Laverny et al. 2006; Abia et al. 2008), thus indicating that the s-process nucleosynthesis is connected to the fluorine production in AGB stars. This implies quite low  $[F/\langle s \rangle]$  values. Lucatello et al. (2011) also found low  $[F/\langle s \rangle]$  in a sample of Galactic s-process rich carbon-enhanced metal-poor stars, thus confirming the results of Abia et al. (2011).

AGB stars are among the most important polluters of the inter-stellar medium. In fact, they eject both light (C, N, F, Na) and heavy elements (see Iben & Renzini 1983; Straniero et al. 2006 for a review). This is the result of the combined action of internal nuclear burning and deep convective mixing episodes taking place during the late part of the AGB, the so-called Thermally Pulsing AGB or TP-AGB phase. The presence of free neutrons in the He-rich intershell of these stars, which is required to synthesize elements heavier than iron, also affects the light elements nucleosynthesis and, among the others, fluorine.

The major source of neutrons in low mass AGB stars is the  $^{13}\text{C}(\alpha, n)^{16}\text{O}$  reaction (Straniero et al. 1995; Gallino et al. 1998), which releases neutrons in the so called  $^{13}\text{C}$ -pocket. It is clear from the '60ties that the  $^{13}\text{C}$  left in the H-shell ashes is not sufficient to account for the observed s-process abundances (Fowler et al. 1955). Thus, the penetration of some protons from the convective envelope into the underlying radiative He-intershell is required during TDU episodes. Later, when the temperature reaches  $10^8$  K, those protons are captured by the abundant  $^{12}\text{C}$  leading to the formation of a thin  $^{13}\text{C}$ -enriched layer, the so-called  $^{13}\text{C}$  pocket. Actually, the mechanism leading to the formation of the  $^{13}\text{C}$  pocket is far from being completely understood. In the last decades, many theories have been proposed (e.g. Sackmann et al. 1974; Iben 1982; Iben & Renzini 1983); most recently, mechanisms as mechanical overshoot (Herwig et al. 1997), gravity waves (Denissenkov & Tout 2003), opacity-induced overshoot (Straniero et al. 2006, see Section 2) and magnetic fields (Trippella et al. 2014) have been invoked. An additional neutron burst is powered by the  $^{22}\text{Ne}(\alpha, n)^{25}\text{Mg}$  reaction, which is activated at the base of the convective zone generated by a TP when the temperature exceeds 300 MK. Such a condition is typical of more massive AGB stars (4-6  $M_{\odot}$ ) (see

Karakas & Lattanzio 2014, for a recent review)

The s-process elements are mainly synthesized by the  $^{13}\text{C}$  burning in radiative conditions in the  $^{13}\text{C}$ -pocket during inter-pulse periods. Neutron captures activated by the  $^{13}\text{C}(\alpha, n)^{16}\text{O}$  also lead to the synthesis of a suitable amount of  $^{15}\text{N}$ , which produces fluorine via the  $^{15}\text{N}(\alpha, \gamma)^{19}\text{F}$  reaction (see Section 3). During the first TPs, a fraction of the  $^{13}\text{C}$  in the  $^{13}\text{C}$ -pocket may survive to the inter-pulse phase. In this case, such  $^{13}\text{C}$  is engulfed into the convective shell generated by the following TP and, thus, it burns in a convective environment (Cristallo et al. 2006). Fluorine is also synthesized starting from the  $^{13}\text{C}$  left by the H-burning shell. This latter  $^{19}\text{F}$  source requires, however, the presence of a quite large amount of C+N+O into the H-rich envelope.

In this paper we investigate fluorine nucleosynthesis in low mass AGB stars by evaluating the effects of the variation of the relevant nuclear reaction rates. In particular, we present the results of an analysis based on an AGB stellar model with initial mass  $M=2 M_{\odot}$  and  $Z = 10^{-3}$ . This model is representative of low-mass AGB stars, i.e. the most promising candidates to reproduce the majority of the observed s-process distributions in AGB stars (see, e.g., Abia et al. 2002). Quite similar results can be obtained for different metallicities or slightly different masses (in the range 1.5-2.5  $M_{\odot}$ ). In this work, larger initial stellar masses (4-6  $M_{\odot}$ ) are not considered since the (eventually) produced fluorine would be efficiently destroyed by  $\alpha$  and neutron captures during TPs (see Section 3), due to the larger temperatures attained by these stars. Moreover, the expected surface s-process distributions of intermediate AGB stars are characterized by low or even negative  $[\text{hs}/\text{ls}]$  indexes and high  $[\text{Rb}/\text{Sr}]$  ratios, in striking contrast with the observed spectra (Abia et al. 2002).

The aim of this work is to identify the nuclear processes whose present uncertainties sizeably affect the theoretical predictions and, thus, deserve further experimental investigations. A similar study of fluorine production in AGB stars was presented almost 10 years ago by Lugaro et al. (2004). With respect to that work we extended the study to a larger number of reactions. Moreover, in the last decade several nuclear cross sections have been measured, or predicted, with improved precision.

In Section II we briefly present the stellar evolutionary code used to calculate the AGB models. In Section III, the fluorine nucleosynthesis path and the nuclear network we use are illustrated. We also critically discuss the uncertainties affecting all the relevant reaction rates. The results of our analysis are illustrated and discussed in Section IV. Our conclusions follow.

## 2. Stellar models

The stellar models presented in this work have been computed with the FUNS (Full Network Stellar) Evolutionary Code (see Straniero et al. 2006, and references therein). This code includes a full nuclear network, with all the relevant isotopes from H up to Bi, the heaviest element synthesized by the s-process, for a total of nearly 500 isotopes linked by more than 1000 nuclear reactions. The coupling of the stellar structure equations with this full network allows to overcome some limitations related to the use of simplified assumptions, to describe stellar phases in which the nucleosynthesis is strongly related to the changes of the physical properties of the stellar environment and vice versa. More details on the nuclear network can be found in Straniero et al. (2006) and Cristallo et al. (2009).

We make use of low temperature C-enhanced molecular opacities (Cristallo et al. 2007) to take into account the modification

<sup>1</sup>  $[\langle s \rangle / \text{Fe}] = 0.5 * (([\text{Sr}/\text{Fe}] + [\text{Y}/\text{Fe}] + [\text{Zr}/\text{Fe}]) / 3 + ([\text{Ba}/\text{Fe}] + [\text{La}/\text{Fe}] + [\text{Nd}/\text{Fe}] + [\text{Sm}/\text{Fe}]) / 4)$ . The two addends represent the surface enrichment of elements belonging to the first peak and second peak of the s-process, respectively.

of the envelope chemical composition determined by the carbon dredge up during the TP-AGB phase.

Concerning mass loss, we adopt a Reimers formula with  $\eta=0.4$  for the pre-AGB evolution, whilst for the AGB we fit the  $\dot{M}$ -Period relation as determined in galactic AGB stars. We follow a procedure similar to that described by Vassiliadis & Wood (1993), but taking into account more recent infrared observations of AGB stars (see Straniero et al. 2006 for the references). We find that our mass-loss rate resembles a moderate Reimers mass loss rate for the first part of the AGB and then switches to a stronger regime toward the tip of the AGB, presenting however a milder slope with respect to the rate proposed by Vassiliadis & Wood (1993).

In our models, in order to handle the discontinuity in the radiative gradient arising during TDU episodes, we introduce at the base of the convective envelope an exponentially decaying profile of convective velocities. This algorithm efficiently works only during TDU episodes, when the H-rich (opaque) envelope approaches the underlying radiative He-rich layers<sup>2</sup>. As a net effect, we obtain deeper TDUs and, as a by-product, the formation of thin  $^{13}\text{C}$  pockets ( $\Delta M < 10^{-3} M_{\odot}$ ). The extension in mass of the  $^{13}\text{C}$  pocket decreases in mass pulse after pulse, following the natural shrinking of the whole He-intershell. Our treatment of the discontinuity in the temperature gradient at the inner border of the convective envelope is based on a free parameter  $\beta$  which has been calibrated in order to maximize the s-process production in low mass AGB stars (see Cristallo et al. 2009 for details).

Of particular relevance for the present paper are some recent updates. All the neutron capture cross sections have been derived from the KADONIS database v 0.3 (Dillmann et al. 2006), except those of Zr isotopes (Tagliente et al. 2010, 2011), Os isotopes (Mosconi et al. 2010) and  $^{197}\text{Au}$  (Lederer et al. 2011). Concerning charged particle reactions involved in the fluorine nucleosynthesis we have considered available new measurements and, more in general, we critically review the available literature (see Section 4). The list of reactions relevant for the nucleosynthesis of  $^{19}\text{F}$  is reported in Table 1.

### 3. Nuclear paths involving $^{19}\text{F}$

The nuclear path leading to fluorine production in low-mass AGB stars is quite complex (Forestini et al. 1992). Within the He-intershell, most of the neutrons released by the  $^{13}\text{C}(\alpha, n)^{16}\text{O}$  reaction during the inter-pulse period are captured by  $^{14}\text{N}$ , via the  $^{14}\text{N}(n, p)^{14}\text{C}$  reaction and, thus, protons are produced. Then, the  $^{14}\text{C}(\alpha, \gamma)^{18}\text{O}$  reaction synthesizes  $^{18}\text{O}$  which, in turn, captures the freshly synthesized protons leading to the production of  $^{15}\text{N}$  via the  $^{18}\text{O}(p, \alpha)^{15}\text{N}$  reaction. This process competes with the main destruction channel of  $^{15}\text{N}$ , i.e. the  $^{15}\text{N}(p, \alpha)^{12}\text{C}$  reaction. Later on, at the development of the following TP,  $^{15}\text{N}$  captures an  $\alpha$  particle producing  $^{19}\text{F}$ . The  $^{15}\text{N}(\alpha, \gamma)^{19}\text{F}$  reaction is therefore the major  $^{19}\text{F}$  production channel.

A further contribution to  $^{15}\text{N}$  production comes from any unburnt  $^{13}\text{C}$  in the  $^{13}\text{C}$  pocket (Cristallo et al. 2009) and from the  $^{13}\text{C}$  left in the H-burning ashes and engulfed in the convective zone generated by a TP, provided a large enough C+N+O abundance in the envelope. Such a  $^{13}\text{C}$  is rapidly burnt at high temperatures leading to the synthesis of  $^{15}\text{N}$  through the same nuclear chain already active in the  $^{13}\text{C}$  pocket. In such a case, however, an additional contribution comes from the

$^{14}\text{N}(\alpha, \gamma)^{18}\text{F}(\beta^+ \nu_e)^{18}\text{O}$  nuclear chain.

A marginal contribution (less than 10%; see, e.g., Gallino et al. 2010) to fluorine nucleosynthesis is given by the  $^{18}\text{O}(n, \gamma)^{19}\text{O}(\beta^- \nu_e)^{19}\text{F}$  nuclear chain.

The  $^{19}\text{F}$  destruction channels are the  $^{19}\text{F}(p, \alpha)^{16}\text{O}$ , the  $^{19}\text{F}(\alpha, p)^{22}\text{Ne}$  and the  $^{19}\text{F}(n, \gamma)^{20}\text{F}$  reactions. In low mass AGB stars, however, the  $^{19}\text{F}$  destruction is rather inefficient, while it could be efficiently activated in higher masses (Lugaro et al. 2004; D’Orazi et al. 2013; Straniero et al. 2014).

### 4. Reaction rates uncertainties

Thanks to the improvements in experimental methods and novel techniques (e.g. Underground Nuclear Physics, Recoil Mass Separator, Trojan Horse etc..) cross sections can be measured at very low energies. This combined with the refinement of the theoretical tools allowed the determination of reaction rates at astrophysically relevant temperature without doing an extrapolation on a wide energy range. In fact, when direct experimental data are not available, the existence of unknown resonance and/or the correct evaluation of resonance parameters and/or interference pattern between different resonances may dramatically change the cross section extrapolations. A general discussion on techniques to extrapolate the cross sections is beyond the aims of this paper (interested readers may refer to Azuma et al. 2010). Nevertheless in the cases where the direct experimental data are relatively close to the Gamow peak energies, the experimental uncertainties may represent a fair description of the reaction rate uncertainties also at relevant energies.

The majority of the most relevant proton radiative captures have been recently remeasured with improved precision extending the data toward, and in some cases well within, the AGB relevant energy range (see, e.g., the underground measurements of the LUNA collaboration of  $^{14}\text{N}(p, \gamma)^{15}\text{O}$  - Imbriani et al. 2005,  $^{15}\text{N}(p, \gamma)^{16}\text{O}$  - Leblanc et al. 2010 and  $^{17}\text{O}(p, \gamma)^{18}\text{F}$  - Di Leva et al. 2014). The experimental uncertainties are relatively small also at relevant energies, i.e. about 10-15% for most of the processes we have considered.

Also most of the (p,  $\alpha$ ) reactions involved in the  $^{19}\text{F}$  synthesis network have been re-measured in the last 10 years, reaching a comparable level of experimental precision. For these processes the uncertainties vary typically between 10 and 30%.

In conclusion, as far as proton-induced processes are concerned, experimental data allow reaction rate calculations at Gamow peak energies without doing large extrapolation of the cross section. In those cases, therefore, the reaction rate uncertainty can be assumed to be robust.

The case of  $\alpha$  capture processes is somewhat different. Due to the much smaller penetrability, the investigated energy range experimentally reached is, for most of the reactions, far from the astrophysically relevant temperatures. Thus, the reaction rates have to be estimated on the basis of cross sections extrapolated to relevant energies by means of models often including resonance parameters evaluated on the basis of gross estimations. As a consequence, experimental uncertainties are much larger, i.e. about 50% in most of the cases. Moreover, it would not be unlikely that new experimental data may produce estimates of  $\alpha$  capture reaction rates significantly different with respect to the current ones, eventually beyond the assumed uncertainties.

In this view, we present the results of two different analyses. In the first one, reaction rates are varied within the  $2\sigma$  uncertainty given by the most recent experiments available in the literature. Then, for few selected cases, we also present a further investi-

<sup>2</sup> We remind that the local radiative gradient (and thus the convective velocity) is proportional to the opacity.

gation, conducted by varying the reaction rates by two order of magnitudes.

The experimental status for the key reactions is briefly outlined below, including some details on the sources of the reaction rates used in this work. The quoted uncertainties at the relevant temperature for the fluorine nucleosynthesis represent  $2\sigma$  standard deviations.

$^{14}\text{N}(\text{p},\gamma)^{15}\text{O}$ . In the last 10 years there have been several experiments that measured this cross section using both direct and indirect methods. In particular, the experiment performed by the LUNA collaboration (Imbriani et al. 2005; Costantini et al. 2009) has reached the lowest energy, about 70 keV, which corresponds to a stellar temperature of about 50 MK. It is worth noting that a reliable extrapolation of the LUNA data to the solar Gamow peak requires the combination of low-energy with high-energy data, namely the results of the LENA experiment at TUNL (Runkle et al. 2005). Additional information is provided by experiments which used indirect methods such as the Doppler shift attenuation method (Bertone et al. 2001; Schürmann et al. 2008), Coulomb excitation (Yamada et al. 2004) and asymptotic normalization coefficients (ANC; Mukhamedzhanov et al. 2003). It is worth noting that the uncertainty on data at high energy affects the low energy extrapolation. For this paper we use the  $S$ -factor recommendation of the recent compilation Solar Fusion II (Adelberger et al. 2011). The uncertainty at relevant temperatures is about 10%.

$^{15}\text{N}(\text{p},\gamma)^{16}\text{O}$ . The low energy cross section of this process is determined by the presence of two broad resonances and by their interference. Recent studies that used indirect methods (Mukhamedzhanov et al. 2008; La Cognata et al. 2009) suggested a cross section significantly lower than previously estimated. A direct experiment (Leblanc et al. 2010; Imbriani et al. 2012) performed in a wide energy window, confirmed that the cross section is about a factor of 2 lower than previously thought. This translates into a significantly lower rate at AGB temperatures. In the present work we use the rate, and the corresponding uncertainty, presented in Leblanc et al. (2010). The uncertainty at relevant temperatures is about 10%.

$^{17}\text{O}(\text{p},\gamma)^{18}\text{F}$ . The cross section of this reaction below  $E_{\text{cm}} \approx 400$  keV is determined by 2 narrow resonances, together with the tails of 2 broad higher energy resonances and the direct capture (DC) component. After the pioneering work of Rolfs (1973) in the seventies, in the last decade several studies (Fox et al. 2005; Chafa et al. 2007; Newton et al. 2010; Hager et al. 2012; Kontos et al. 2012; Scott et al. 2012) have determined the reaction rate with improving precision. Nevertheless, at the temperatures relevant for AGB nucleosynthesis, the reaction rate is dominated by the lowest energy resonance,  $E_{\text{cm}} = 65$  keV, that is too weak to be directly measured with the current experiment possibilities. For the present work we use the reaction rate determination by Di Leva et al. (2014) based on the measurement of the LUNA collaboration. The uncertainty at relevant temperatures is about 15%.

$^{18}\text{O}(\text{p},\gamma)^{19}\text{F}$ . Also in this case the presence of several low energy states influences the determination of the cross section. In particular, the  $E_{\text{cm}} = 150$  keV broad resonance and the direct capture dominate the reaction rate at the astrophysically relevant temperature for AGB nucleosynthesis. Wiescher et al. (1980) and Vogelaar et al. (1990) have directly determined the magnitude of all the relevant states, down to  $E_{\text{cm}} = 89$  keV. For the present work we adopt the reaction rate given in the recent compilation by Iliadis et al. (2010). The uncertainty at relevant temperatures is about 10%.

$^{15}\text{N}(\text{p},\alpha)^{12}\text{C}$ . The reaction rate of this process, at the temperatures of interest for this study, is mostly determined by a resonance at  $E_{\text{cm}} \approx 100$  keV. The cross section was directly determined by Redder et al. (1982). More recently, this reaction has been investigated again using the indirect approach of the Trojan Horse Method (THM; La Cognata et al. 2007), yielding results similar to Redder et al. (1982), for both the central value and the uncertainty. For the present work we use the reaction rate reported in the NACRE compilation Angulo et al. (1999). The uncertainty at relevant temperatures is about 10%.

$^{17}\text{O}(\text{p},\alpha)^{14}\text{N}$ . Several experiments (Chafa et al. 2007; Newton et al. 2010; Moazen et al. 2007) determined the magnitude of most of the several resonances that influence the rate of this reaction. As for the  $^{17}\text{O}(\text{p},\gamma)^{18}\text{F}$  the presence of the  $E_{\text{cm}} = 65$  keV resonance, directly at the astrophysically relevant energy, makes the reaction rate determination difficult and the uncertainty is correspondingly large. For the present work we adopt the value suggested by Iliadis et al. (2010). The uncertainty at relevant temperatures is about 20%.

$^{18}\text{O}(\text{p},\alpha)^{15}\text{N}$ . The low energy determination of this cross section is complicated by the tail of high energy broad resonances and by the presence of several low energy states (Lorenz-Wirzba et al. 1979). Recently La Cognata et al. (2010) have remeasured with the THM this cross section, strongly reducing the corresponding uncertainty. For the present calculations we use the reaction rate provided by Iliadis et al. (2010). The uncertainty at relevant temperatures is up to 30%.

$^{19}\text{F}(\text{p},\alpha)^{16}\text{O}$ . The situation is very similar to the previous case. The presence of very low energy resonances makes direct determination of the cross section very difficult. An indirect experiment using the THM (La Cognata et al. 2011) has observed the presence of resonances not seen before in this process at energies corresponding to typical AGB temperatures, thus implying a significant increase of the reaction rate. Thus, the reaction rate proposed by La Cognata et al. (2011) is used in our calculations. The uncertainty at relevant temperatures is about 30%.

$^{14}\text{C}(\alpha,\gamma)^{18}\text{O}$ . The determination of this cross section is not easy, because of the difficulty of  $^{14}\text{C}$  targets or beams production. Few direct experiments have been performed to determine this cross section (Görres et al. 1992). Recently the cross section was determined through indirect techniques by Johnson et al. (2009). A better knowledge of several resonances was achieved with a significant improvement in the uncertainty in the reaction rate at temperatures lower than typical for AGBs. In the temperature window relevant for our study there is a general agreement between the reaction rates provided by Görres et al. (1992) and Johnson et al. (2009). In our calculations we used the reaction rate given by Lugaro et al. (2004), which is based on the Görres et al. (1992) data with the exception of the spectroscopic factor of the 6.2 MeV state, for which they used a higher value. The uncertainty at relevant temperatures is about 50%.

$^{18}\text{O}(\alpha,\gamma)^{22}\text{Ne}$ . The determination of this reaction rate is particularly complex and several experiments have been done to collect all the necessary information. The determination is relatively uncertain at lower energy. We followed the prescriptions by Iliadis et al. (2010). The uncertainty at relevant temperatures is about 50%.

$^{19}\text{F}(\alpha,\text{p})^{20}\text{Ne}$ . The only experiment available has been done by Ugalde et al. (2008). These authors have measured this cross section, using an  $\alpha$  beam and a F solid target between  $E_{\text{cm}} = 700$  and 1600 keV, still far from the relevant astrophysical energy. The uncertainty at relevant temperatures is up to 50%.

$^{13}\text{C}(\alpha,\text{n})^{16}\text{O}$ . This reaction is the major neutron source in low mass AGB star and releases neutrons in radiative condi-

tions during the inter-pulse period at temperatures  $T \sim 10^8$  K. The  $^{13}\text{C}(\alpha, n)^{16}\text{O}$  reaction has been studied over a wide energy range, but none of the existing experimental investigations has fully covered the relevant astrophysical energies. The present low energy limit in a direct experiment is  $E_{\text{cm}} = 220$  keV, while the astrophysical relevant energy is between  $\sim 150$  and  $250$  keV. This means that the cross section at the typical AGB temperatures has to be extrapolated from the data through model predictions. For our calculation we have used the reaction rate derived by Heil et al. (2008). The uncertainty at relevant temperatures is up to 50%.

$^{14}\text{N}(\alpha, \gamma)^{18}\text{F}$ . The rate of the  $^{14}\text{N}(\alpha, \gamma)^{18}\text{F}$  reaction is dominated by the contribution of a  $J^\pi = 1^-$  resonance at  $E_{\text{cm}} = 572$  keV for temperatures between 0.1 GK and 0.5 GK. For higher temperatures the contributions of resonances at higher energies ( $E_{\text{cm}} = 883, 1088, 1189$  and  $1258$  keV) become more important. Below 0.1 GK additional contributions are possible from the low-energy tail of the 445 keV resonance, the DC component, and the  $J^\pi = 4^+$  resonance at 237 keV. The lowest directly measured resonance is the one at 445 keV, which has been measured together with the resonance at 1136 keV (Görres et al. 2000a).

The strength of the  $E_{\text{cm}} = 237$  keV resonance has never been measured. It has been argued (Görres et al. 2000a) that it is extremely small ( $\omega\gamma \sim 1.5 \cdot 10^{-18}$  keV), far below present experimental measurement possibilities.

The DC for this reaction is only theoretically estimated. It is supposed to be  $\sim 0.7 - 0.8$  keVb, as calculated from spectroscopic factors using some crude approximations (see comments in Iliadis et al. 2010). The uncertainty at relevant temperatures is up to 20%.

$^{15}\text{N}(\alpha, \gamma)^{19}\text{F}$ . The rate of the  $^{15}\text{N}(\alpha, \gamma)^{19}\text{F}$  reaction is dominated by resonance contributions of several low-lying states in  $^{19}\text{F}$ . Wilmes et al. (2002) measured all the resonance strengths in the energy window 0.6 MeV to 2.7 MeV. Nevertheless at astrophysical relevant energies contributions from the  $E_{\text{cm}} = 364$  keV, 536 keV and 542 keV resonances are important.

The strength of the 364 keV resonance has been measured indi-

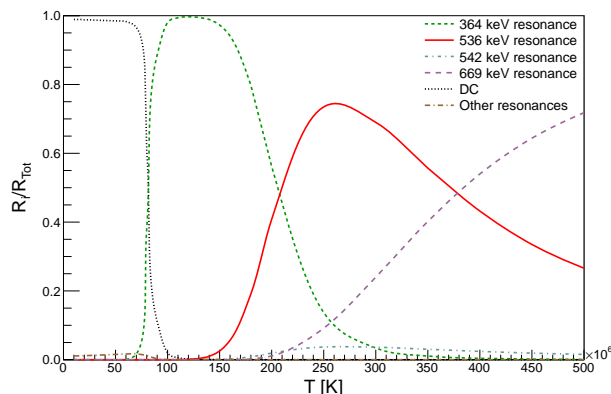


**Fig. 1.** Fractional contribution of the different resonances and the DC to the  $^{15}\text{N}(\alpha, \gamma)^{19}\text{F}$  reaction rate.

rectly de Oliveira et al. (1996) using the  $^{15}\text{N}(^7\text{Li}, t)^{19}\text{F}$  reaction at 28 MeV, the uncertainty associated with the model used to derive the results is estimated to be a factor of 2. This resonance directly influences the determination of the reaction rate for temperatures lower than 200 MK. Thus, a direct measurement of its strength is of great importance. In Figure 1 we show the contributions of the resonances and the DC to the total rate versus the

temperature for the  $^{15}\text{N}(\alpha, \gamma)^{19}\text{F}$ . The uncertainty ranges from 15% at 250 MK, up to a factor 2 below 180 MK (see Table 2).

Considering the minor contribution of the  $^{18}\text{O}(n, \gamma)^{19}\text{O}$  reaction to  $^{19}\text{F}$  production we exclude this reaction from our analysis. Similarly, we do not take into account variations of the  $^{19}\text{F}(n, \gamma)^{20}\text{F}$ , since in low mass stars this reaction is not efficiently activated.

A list of the studied reaction rates is provided in Table 2 (column 1). Upper and lower percentage cross section uncertainties ( $2\sigma$ ) are reported at  $T=1 \times 10^8$  K and  $T=2.5 \times 10^8$  K (column 2-3 and 4-5). These are the typical temperatures of the nucleosynthesis occurring in the  $^{13}\text{C}$  pockets and in the convective shells generated by thermal pulses, respectively.

## 5. Results

As a first step, we compute a model by using the new set of reaction rates reported in Table 1 (hereinafter ST case). We select a model with initial mass  $M=2 M_\odot$  and  $Z = 10^{-3}$  ( $[\text{Fe}/\text{H}]=-1.15$ ), considered as representative of low mass AGB stars. The initial He abundance is set to 0.245; the distribution of metals is assumed to be solar scaled and taken from Lodders (2003). No  $\alpha$ -element enhancements are considered. The mixing length parameter ( $\alpha_{\text{ml}}$ ) has been calibrated by computing a standard Solar Model and its value is set to 2.1 (Piersanti et al. 2007). The evolution of this model has been stopped after the last TDU, when the core has a mass of  $0.686 M_\odot$  and the mass of the remaining convective envelope is smaller than  $7 \times 10^{-3} M_\odot$ . During its evolution, this model experience 20 thermal pulses, 19 of which followed by TDU. For more details we refer to Cristallo et al. (2009).

With respect to a model computed with the previous version of the network, we obtain a reduction of the surface  $[\text{F}/\text{Fe}]$  of 29% (and a corresponding reduction of the  $[\text{F}/\langle s \rangle]$  of 22%). This result is mainly ascribed to the strongly reduced rate (about a factor 1000 at relevant temperatures) of the  $^{14}\text{C}(\alpha, \gamma)^{18}\text{O}$  reaction (Lugaro et al. 2004) with respect to the rate adopted in our previous calculations (Caughlan & Fowler 1988). Such a low rate limits the local increase of  $^{18}\text{O}$ . Later on, part of this  $^{14}\text{C}$  is dredged up to the surface and it decays to  $^{14}\text{N}$ , thus not directly contributing to fluorine nucleosynthesis within the He-intershell.

Then, we assume as a reference case the model computed with such a new nuclear network (hereafter ST case) and we vary one at a time all the reactions reported in Table 2 in both directions (upper and lower limits). For each varied reaction, we compute the evolution of the star from the end of the core He-burning phase up to the tip of the AGB phase.

### 5.1. $2\sigma$ analysis

We firstly studied the effects on fluorine nucleosynthesis due to variations of the relevant reaction rates by changing them within  $2\sigma$  values, as derived from the extant literature.

Results are shown in Table 2, where we tabulate the final (i.e. after the last TDU) surface  $[\text{F}/\text{Fe}]$  and  $[\text{F}/\langle s \rangle]$  percentage differences with respect to our ST case. For both quantities we provide variations corresponding to upper and lower rates. From the values reported in Table 2 it comes out that the variations of key reaction rates within  $2\sigma$  have little effect on the final fluorine surface abundances and  $[\text{F}/\langle s \rangle]$  ratios. Largest variations are found for the  $^{14}\text{N}(p, \gamma)^{15}\text{O}$ , the  $^{19}\text{F}(\alpha, p)^{22}\text{Ne}$  and the  $^{13}\text{C}(\alpha, n)^{16}\text{O}$  reactions. However, such differences in the final

surface fluorine abundance are definitely lower than the errors currently affecting spectroscopic observations (at least a factor 2).

## 5.2. Exploration above current experimental uncertainties

In order to better evaluate the sensitivity of  $^{19}\text{F}$  nucleosynthesis to larger variations of selected reaction rates, we run some additional tests by varying the cross section of  $\alpha$  capture processes well beyond the currently quoted uncertainties. The computed tests are listed in Table 3, where we report:

- scaling factors  $sf$  (i.e. the ratio of the modified rate with respect to the reference case);
- corresponding final surface  $^{19}\text{F}$  ratios with respect to the reference case ( $R(^{19}\text{F}) = {}^{19}\text{F}_{\text{test}}/{}^{19}\text{F}_{ST}$ );
- corresponding final surface  $F/\langle s \rangle$  ratios with respect to the reference case ( $R(F/\langle s \rangle) = (F/\langle s \rangle)_{\text{test}}/(F/\langle s \rangle)_{ST}$ ).

Among the studied rates, the  $^{14}\text{C}(\alpha,\gamma)^{18}\text{O}$  and the  $^{18}\text{O}(\alpha,\gamma)^{22}\text{Ne}$  show the lowest variations. Large changes of the  $^{14}\text{N}(\alpha,\gamma)^{18}\text{F}$  and the  $^{13}\text{C}(\alpha,n)^{16}\text{O}$  reactions imply small, but appreciable, differences in the final fluorine surface abundances. The remaining two rates, i.e. the  $^{15}\text{N}(\alpha,\gamma)^{19}\text{F}$  and the  $^{19}\text{F}(\alpha,p)^{22}\text{Ne}$  are able to reduce by a factor of 10 the surface  $^{19}\text{F}$  abundance and, thus, deserve a more careful analysis.

### 5.2.1. The revisited $^{15}\text{N}(\alpha,\gamma)^{19}\text{F}$

Interestingly enough, the model with a strongly reduced  $^{15}\text{N}(\alpha,\gamma)^{19}\text{F}$  roughly matches the observed  $[F/\langle s \rangle]$  ratios found at low metallicity by Abia et al. (2011). Note that, as we already remarked, the  $^{15}\text{N}(\alpha,\gamma)^{19}\text{F}$  rate is strongly influenced by the presence of the 364 keV resonance, whose intensity is affected by a very large uncertainty. The contribution from the DC component is also difficult to evaluate at the present status of the experimental knowledge. Therefore, although very unlikely, the explored scenario is not impossible from a nuclear point of view. Nevertheless, a very low value of the  $^{15}\text{N}(\alpha,\gamma)^{19}\text{F}$  reaction would not allow AGB stars to synthesize fluorine at solar-like metallicities, in contradiction with observations (Abia et al. 2010). As already recalled, however, preliminary studies based on a recent reduction of the adopted excitation energies of HF molecular transitions seem to lead to a consistent decrease of the observed fluorine surface abundances in solar-like metallicity AGB stars (Abia et al., in preparation).

A revision of this reaction rate looks therefore mandatory, in order to minimize the uncertainty on  $^{19}\text{F}$  nucleosynthesis related to this nuclear process. We will clarify this issue in the near future, when we will directly measure the strength of the 364 keV resonance and the intensity of the DC component, using the ERNA recoil separator (Schürmann et al. 2005; di Leva et al. 2009; Di Leva et al. 2012).

### 5.2.2. The revisited $^{19}\text{F}(\alpha,p)^{22}\text{Ne}$

The only other  $\alpha$  capture process able to significantly change the surface fluorine abundances in low mass AGB stars is the  $^{19}\text{F}(\alpha,p)^{22}\text{Ne}$ . In state-of-the-art modelling, this reaction rate is expected to efficiently work in stars with larger masses ( $M \geq 4 - 5M_{\odot}$ <sup>3</sup>). However, a deep revision of this rate cannot be ex-

<sup>3</sup> Note that, as already highlighted in the Introduction, this class of objects cannot reproduce the observed AGB s-process distributions.

cluded from first principles. In fact, the  $^{19}\text{F}(\alpha,p)^{22}\text{Ne}$  cross section is characterized by many broad resonances tailing into the low-energy range. Possible additional resonance contributions in that excitation range were predicted, on the basis of  $^{23}\text{Na}$  compound nuclear level structure data. As discussed in Section 4, experimental data are still far from the relevant astrophysical energies. The uncertainty is mostly due to the different energy dependence of the cross section predicted by different models. We intend to clarify this point by realizing a direct measurement of this cross section at energy lower than  $E_{cm} = 660$  keV, using a fluorine beam impinging into an  $\alpha$  jet gas target surrounded by particle detectors.

## 6. Conclusions

In this paper we investigated the effects that nuclear reaction rates have on the fluorine production in low mass AGB stars. We found minor variations in the final surface  $^{19}\text{F}$  abundance (less than 10%) when varying the rates within  $2\sigma$  standard deviations. However, some  $\alpha$  capture reactions may change well beyond the current accepted uncertainties, due to the lack of knowledge about the strengths of nuclear resonances at astrophysical relevant energies. Thus, we investigated further possible, although unlikely, scenarios in which we varied some  $\alpha$  capture rates by a factor 100. We found that the largest variations are obtained by reducing the  $^{15}\text{N}(\alpha,\gamma)^{19}\text{F}$  rate or by increasing the  $^{19}\text{F}(\alpha,p)^{22}\text{Ne}$  rate. Both reactions have poorly known resonances at astrophysical energies. We plan to experimentally investigate both cross sections in the future directly measuring the strengths of their resonances.

*Acknowledgements.* This work was supported by Italian Grants RBFR08549F-002 (FIRB 2008 program), PRIN-INAF 2011 project "Multiple populations in Globular Clusters: their role in the Galaxy assembly", PRIN-MIUR 2012 "Nucleosynthesis in AGB stars: an integrated approach" project (20128PCN59) and from Spanish grants AYA2008-04211-C02-02 and AYA-2011-22460.

## References

- Abia, C., Cunha, K., Cristallo, S., et al. 2010, *Astrophys. J. Lett.*, 715, L94  
 Abia, C., Cunha, K., Cristallo, S., et al. 2011, *Astrophys. J. Lett.*, 737, L8  
 Abia, C., de Laverny, P., & Wahlin, R. 2008, *Astron. & Astrophys.*, 481, 161  
 Abia, C., Domínguez, I., Gallino, R., et al. 2002, *ApJ*, 579, 817  
 Abia, C., Recio-Blanco, A., de Laverny, P., et al. 2009, *ApJ*, 694, 971  
 Adelberger, E. G., García, A., Robertson, R. G. H., et al. 2011, *Reviews of Modern Physics*, 83, 195  
 Angulo, C., Arnould, M., Rayet, M., et al. 1999, *Nuclear Physics A*, 656, 3  
 Azuma, R. E., Uberseder, E., Simpson, E. C., et al. 2010, *Phys. Rev. C*, 81, 045805  
 Bertone, P. F., Champagne, A. E., Powell, D. C., et al. 2001, *Physical Review Letters*, 87, 152501  
 Caughlan, G. R. & Fowler, W. A. 1988, *Atomic Data and Nuclear Data Tables*, 40, 283  
 Chafa, A., Tatischeff, V., Aguer, P., et al. 2007, *Phys. Rev. C*, 75, 035810  
 Costantini, H., Formicola, A., Imbriani, G., et al. 2009, *Reports on Progress in Physics*, 72, 086301  
 Cristallo, S., Gallino, R., Straniero, O., Piersanti, L., & Domínguez, I. 2006, *Mem. Soc. Astron. Italiana*, 77, 774  
 Cristallo, S., Piersanti, L., Straniero, O., et al. 2011, *Astrophys. J. Suppl.*, 197, 17  
 Cristallo, S., Straniero, O., Gallino, R., et al. 2009, *ApJ*, 696, 797  
 Cristallo, S., Straniero, O., Lederer, M. T., & Aringer, B. 2007, *ApJ*, 667, 489  
 de Laverny, P., Abia, C., Domínguez, I., et al. 2006, *Astron. & Astrophys.*, 446, 1107  
 de Oliveira, F., Coc, A., Aguer, P., et al. 1996, *Nuclear Physics A*, 597, 231  
 Denissenkov, P. A. & Tout, C. A. 2003, *MNRAS*, 340, 722  
 di Leva, A., Gialanella, L., Kunz, R., et al. 2009, *Physical Review Letters*, 102, 232502  
 Di Leva, A., Pezzella, A., De Cesare, N., et al. 2012, *Nuclear Instruments and Methods in Physics Research A*, 689, 98

- Di Leva, A., Scott, D. A., Caciolli, A., et al. 2014, *Phys. Rev. C*, 89, 015803
- Di Leva, A., Scott, D. A., Caciolli, A., et al. 2014, *Phys. Rev. C*, 89, 015803
- Dillmann, I., Heil, M., Käppeler, F., et al. 2006, in *American Institute of Physics Conference Series*, Vol. 819, *Capture Gamma-Ray Spectroscopy and Related Topics*, ed. A. Woehr & A. Aprahamian, 123–127
- D’Orazi, V., Lucatello, S., Lugaro, M., et al. 2013, *ApJ*, 763, 22
- Drotleff, H. W., Denker, A., Knee, H., et al. 1993, *ApJ*, 414, 735
- Federman, S. R., Sheffer, Y., Lambert, D. L., & Smith, V. V. 2005, *ApJ*, 619, 884
- Forestini, M., Goriely, S., Jorissen, A., & Arnould, M. 1992, *Astron. & Astrophys.*, 261, 157
- Formicola, A., Imbriani, G., Costantini, H., et al. 2004, *Physics Letters B*, 591, 61
- Fowler, W. A., Burbidge, G. R., & Burbidge, E. M. 1955, *ApJ*, 122, 271
- Fox, C., Iliadis, C., Champagne, A. E., et al. 2005, *Phys. Rev. C*, 71, 055801
- Gallino, R., Arlandini, C., Busso, M., et al. 1998, *ApJ*, 497, 388
- Gallino, R., Bisterzo, S., Cristallo, S., & Straniero, O. 2010, *Mem. of the Soc. Astr. It.*, 81, 998
- Giesen, U., Browne, C. P., Görres, J., et al. 1994, *Nuclear Physics A*, 567, 146
- Görres, J., Arlandini, C., Giesen, U., et al. 2000a, *Phys. Rev. C*, 62, 055801
- Görres, J., Arlandini, C., Giesen, U., et al. 2000b, *Phys. Rev. C*, 62, 055801
- Görres, J., Graff, S., Wiescher, M., et al. 1992, *Nuclear Physics A*, 548, 414
- Hager, U., Buchmann, L., Davids, B., et al. 2012, *Phys. Rev. C*, 85, 035803
- Heil, M., Detwiler, R., Azuma, R. E., et al. 2008, *Phys. Rev. C*, 78, 025803
- Herwig, F., Bloeker, T., Schoenberner, D., & El Eid, M. 1997, *A&A*, 324, L81
- Iben, Jr., I. 1982, *ApJ*, 260, 821
- Iben, Jr., I. & Renzini, A. 1983, *Annual Rev. of Astron. and Astroph.*, 21, 271
- Iliadis, C., Longland, R., Champagne, A. E., Coc, A., & Fitzgerald, R. 2010, *Nuclear Physics A*, 841, 31
- Imbriani, G., Costantini, H., Formicola, A., et al. 2005, *European Physical Journal A*, 25, 455
- Imbriani, G., deBoer, R. J., Best, A., et al. 2012, *Phys. Rev. C*, 85, 065810
- Johnson, E. D., Rogachev, G. V., Mitchell, J., Miller, L., & Kemper, K. W. 2009, *Phys. Rev. C*, 80, 045805
- Jönsson, H., Ryde, N., Harper, G. M., et al. 2014, *Astron. & Astrophys.*, 564, A122
- Jorissen, A., Smith, V. V., & Lambert, D. L. 1992, *Astron. & Astrophys.*, 261, 164
- Karakas, A. I. & Lattanzio, J. C. 2014, *ArXiv e-prints*
- Kobayashi, C., Izutani, N., Karakas, A. I., et al. 2011, *Astrophys. J. Lett.*, 739, L57
- Kontos, A., Görres, J., Best, A., et al. 2012, *Phys. Rev. C*, 86, 055801
- La Cognata, M., Goldberg, V. Z., Mukhamedzhanov, A. M., Spitaleri, C., & Tribble, R. E. 2009, *Phys. Rev. C*, 80, 012801
- La Cognata, M., Mukhamedzhanov, A. M., Spitaleri, C., et al. 2011, *Astrophys. J. Lett.*, 739, L54
- La Cognata, M., Romano, S., Spitaleri, C., et al. 2007, *Phys. Rev. C*, 76, 065804
- La Cognata, M., Spitaleri, C., & Mukhamedzhanov, A. M. 2010, *ApJ*, 723, 1512
- Leblanc, P. J., Imbriani, G., Görres, J., et al. 2010, *Phys. Rev. C*, 82, 055804
- Lederer, C., Colonna, N., Domingo-Pardo, C., et al. 2011, *Phys. Rev. C*, 83, 034608
- Lodders, K. 2003, *ApJ*, 591, 1220
- Lorenz-Wirzba, H., Schmalbrock, P., Trautvetter, H. P., et al. 1979, *Nuclear Physics A*, 313, 346
- Lucatello, S., Masseron, T., Johnson, J. A., Pignatari, M., & Herwig, F. 2011, *ApJ*, 729, 40
- Lugaro, M., Ugalde, C., Karakas, A. I., et al. 2004, *ApJ*, 615, 934
- Meynet, G. & Arnould, M. 2000, *Astron. & Astroph.*, 355, 176
- Moazen, B. H., Bardayan, D. W., Blackmon, J. C., et al. 2007, *Phys. Rev. C*, 75, 065801
- Mosconi, M., Fujii, K., Mengoni, A., et al. 2010, *Phys. Rev. C*, 82, 015802
- Mukhamedzhanov, A. M., Bém, P., Brown, B. A., et al. 2003, *Phys. Rev. C*, 67, 065804
- Mukhamedzhanov, A. M., Bém, P., Burjan, V., et al. 2008, *Phys. Rev. C*, 78, 015804
- Newton, J. R., Iliadis, C., Champagne, A. E., et al. 2010, *Phys. Rev. C*, 81, 045801
- Palacios, A., Arnould, M., & Meynet, G. 2005, *Astron. & Astrophys.*, 443, 243
- Piersanti, L., Straniero, O., & Cristallo, S. 2007, *A&A*, 462, 1051
- Redder, A., Becker, H. W., Lorenz-Wirzba, H., et al. 1982, *Zeitschrift für Physik A Hadrons and Nuclei*, 305, 325
- Rolfs, C. 1973, *Nuclear Physics A*, 217, 29
- Runkle, R. C., Champagne, A. E., Angulo, C., et al. 2005, *Physical Review Letters*, 94, 082503
- Sackmann, I.-J., Smith, R. L., & Despain, K. H. 1974, *ApJ*, 187, 555
- Schürmann, D., di Leva, A., Gialanella, L., et al. 2005, *European Physical Journal A*, 26, 301
- Schürmann, D., Kunz, R., Lingner, I., et al. 2008, *Phys. Rev. C*, 77, 055803
- Scott, D. A., Caciolli, A., Di Leva, A., et al. 2012, *Physical Review Letters*, 109, 202501
- Straniero, O., Cristallo, S., & Piersanti, L. 2014, *ApJ*, 785, 77
- Straniero, O., Gallino, R., Busso, M., et al. 1995, *Astrophys. J. Lett.*, 440, L85
- Straniero, O., Gallino, R., & Cristallo, S. 2006, *Nuclear Physics A*, 777, 311
- Tagliente, G., Milazzo, P. M., Fujii, K., et al. 2010, *Phys. Rev. C*, 81, 055801
- Tagliente, G., Milazzo, P. M., Fujii, K., et al. 2011, *Phys. Rev. C*, 84, 055802
- Trippella, O., Busso, M., Maiorca, E., Käppeler, F., & Palmerini, S. 2014, *ApJ*, 787, 41
- Ugalde, C. 2005, PhD thesis, University of Notre Dame
- Ugalde, C., Azuma, R. E., Couture, A., et al. 2008, *Phys. Rev. C*, 77, 035801
- Vassiliadis, E. & Wood, P. R. 1993, *ApJ*, 413, 641
- Vogelaar, R. B., Wang, T. R., Kellogg, S. E., & Kavanagh, R. W. 1990, *Phys. Rev. C*, 42, 753
- Wiescher, M., Becker, H. W., Görres, J., et al. 1980, *Nuclear Physics A*, 349, 165
- Wilmes, S., Wilmes, V., Staudt, G., Mohr, P., & Hammer, J. W. 2002, *Phys. Rev. C*, 66, 065802
- Woosley, S. E. & Haxton, W. C. 1988, *Nature*, 334, 45
- Yamada, K., Motobayashi, T., Akiyoshi, H., et al. 2004, *Physics Letters B*, 579, 265





**Table 1.** Sources of the reaction rates relevant for fluorine nucleosynthesis: "Old source" list corresponds to the network used in Straniero et al. 2006 and Cristallo et al. 2009; "New source" list refers to the present work.

Reaction rate	Old Source	New Source
<b>1 Proton captures</b>		
$^{14}\text{N}(p,\gamma)^{15}\text{O}$	Formicola et al. (2004)	Adelberger et al. (2011)
$^{15}\text{N}(p,\gamma)^{16}\text{O}$	Angulo et al. (1999)	Leblanc et al. (2010)
$^{17}\text{O}(p,\gamma)^{18}\text{F}$	Angulo et al. (1999)	Scott et al. (2012)
$^{18}\text{O}(p,\gamma)^{19}\text{F}$	Angulo et al. (1999)	Iliadis et al. (2010)
$^{15}\text{N}(p,\alpha)^{12}\text{C}$	Angulo et al. (1999)	Angulo et al. (1999)
$^{17}\text{O}(p,\alpha)^{14}\text{N}$	Angulo et al. (1999)	Iliadis et al. (2010)
$^{18}\text{O}(p,\alpha)^{15}\text{N}$	Angulo et al. (1999)	Iliadis et al. (2010)
$^{19}\text{F}(p,\alpha)^{16}\text{O}$	Angulo et al. (1999)	La Cognata et al. (2011)
<b><math>\alpha</math> captures</b>		
$^{14}\text{C}(\alpha,\gamma)^{18}\text{O}$	Caughlan & Fowler (1988)	Lugaro et al. (2004)
$^{14}\text{N}(\alpha,\gamma)^{18}\text{F}$	Görres et al. (2000b)	Iliadis et al. (2010)
$^{15}\text{N}(\alpha,\gamma)^{19}\text{F}$	Angulo et al. (1999)	Iliadis et al. (2010)
$^{18}\text{O}(\alpha,\gamma)^{22}\text{Ne}$	Giesen et al. (1994)	Iliadis et al. (2010)
$^{19}\text{F}(\alpha,p)^{22}\text{Ne}$	Ugalde (2005)	Ugalde et al. (2008)
$^{13}\text{C}(\alpha,n)^{16}\text{O}$	Drotleff et al. (1993)	Heil et al. (2008)

**Table 2.**  $2\sigma$  percentage cross section upper and lower uncertainties at  $T=1 \times 10^8$  K and  $T=2.5 \times 10^8$  K and corresponding percentage fluorine surface variations. See text for details.

Reaction rate	$2\sigma (T_8 = 1)$		$2\sigma (T_8 = 2.5)$		$\Delta [\text{F}/\text{Fe}]$ (% var.)		$\Delta [\text{F}/\langle s \rangle]$ (% var.)	
	Upper	Lower	Upper	Lower	Upper	Lower	Upper	Lower
$^{14}\text{N}(p,\gamma)^{15}\text{O}$	10	10	8	8	-3	+5	-3	+3
$^{15}\text{N}(p,\gamma)^{16}\text{O}$	15	15	15	15	-1	-2	-3	-2
$^{17}\text{O}(p,\gamma)^{18}\text{F}$	15	15	20	20	0	-2	-3	0
$^{18}\text{O}(p,\gamma)^{19}\text{F}$	30	30	30	30	-2	-3	-1	-3
$^{15}\text{N}(p,\alpha)^{12}\text{C}$	20	20	15	15	-3	+1	-3	-3
$^{17}\text{O}(p,\alpha)^{14}\text{C}$	15	15	6	6	-2	-2	-1	0
$^{18}\text{O}(p,\alpha)^{15}\text{N}$	8	8	8	8	+1	-2	+3	-1
$^{19}\text{F}(p,\alpha)^{16}\text{O}$	35	35	35	35	0	-1	-4	-4
$^{14}\text{C}(\alpha,\gamma)^{18}\text{O}$	100	84	100	62	-2	0	-3	-2
$^{14}\text{N}(\alpha,\gamma)^{18}\text{F}$	20	20	10	10	-1	-1	+3	-1
$^{15}\text{N}(\alpha,\gamma)^{19}\text{F}$	100	50	15	15	-3	-2	0	+5
$^{18}\text{O}(\alpha,\gamma)^{22}\text{Ne}$	70	50	70	50	-3	+1	-4	-5
$^{19}\text{F}(\alpha,p)^{22}\text{Ne}$	100	100	50	50	-5	+2	-2	+4
$^{13}\text{C}(\alpha,n)^{16}\text{O}$	25	25	25	25	-3	+7	-1	+3

 $T_8$ : temperature in units of  $10^8$  K

**Table 3.** Scaling factors  $sf$  of the computed tests with the corresponding  $^{19}\text{F}$  and  $\text{F}/\langle s \rangle$  surface ratios with respect to the reference case. See text for details.

Reaction rate	$sf$	$\text{R}(^{19}\text{F})$	$\text{R}(\text{F}/\langle s \rangle)$
$^{13}\text{C}(\alpha, \text{n})^{16}\text{O}$	0.01	4.70	2.80
$^{13}\text{C}(\alpha, \text{n})^{16}\text{O}$	100	0.62	0.67
$^{14}\text{C}(\alpha, \gamma)^{18}\text{O}$	0.01	1.03	1.59
$^{14}\text{C}(\alpha, \gamma)^{18}\text{O}$	100	1.04	1.61
$^{14}\text{N}(\alpha, \gamma)^{18}\text{F}$	0.01	3.03	5.14
$^{14}\text{N}(\alpha, \gamma)^{18}\text{F}$	100	0.64	1.10
$^{15}\text{N}(\alpha, \gamma)^{19}\text{F}$	0.01	0.11	0.12
$^{15}\text{N}(\alpha, \gamma)^{19}\text{F}$	100	0.96	1.50
$^{18}\text{O}(\alpha, \gamma)^{22}\text{Ne}$	0.01	2.21	2.01
$^{18}\text{O}(\alpha, \gamma)^{22}\text{Ne}$	100	0.52	0.52
$^{19}\text{F}(\alpha, \text{p})^{22}\text{Ne}$	0.01	1.05	1.19
$^{19}\text{F}(\alpha, \text{p})^{22}\text{Ne}$	100	0.08	0.14